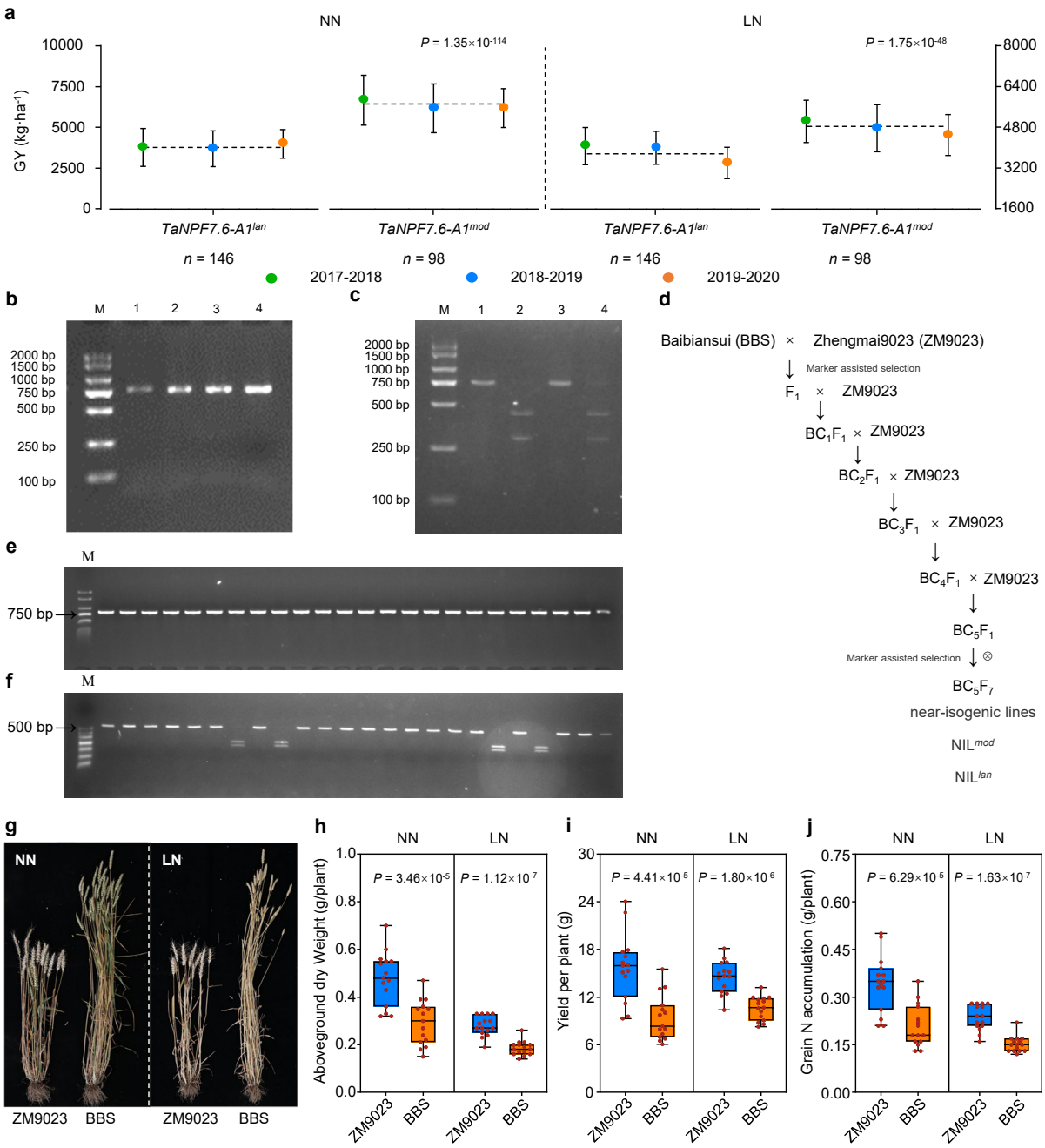

Supplementary Fig. 1 Comparison of the GY between TaNPF7.6-A1 two alleles and genetic construction of NILs. a Comparison of the GY between *TaNPF7.6-A1* two alleles under NN and LN fields in 2017-2018 (green, left), 2018-2019 (blue, middle), and 2019-2020 (orange, right). The data used for calculation derived from experiments shown in Fig 1g-1h, and the dotted lines represent the domain-averaged values. **b-c** A CAPS marker developed from a single-nucleotide polymorphism (T/C) at the 35562744(+) bp on Chromosome 1A of the IWGSCv1.0 using the restriction enzyme *Sac* II, and was further used to track *TaNPF7.6-A1* and its homozygous or heterozygous status in molecular breeding, *TaNPF7.6-A1*^{lan} can be cleaved by restriction enzyme *Sac* II, while *TaNPF7.6-A1*^{mod} cannot. PCR amplification of 1: Zhengmai9023 (ZM9023), 2: Baibiansui (BBS), 3: Zhengmai1860 (ZM1860), 4: Ermangmai (EMM) using CAPS marker (**b**), PCR products of 1: ZM9023, 2: BBS, 3: ZM1860, 4: EMM were digested using the restriction enzyme *Sac* II (**c**). **d** Genetic construction of NILs with *TaNPF7.6-A1*^{lan} and *TaNPF7.6-A1*^{mod}. **e-f** PCR amplification of certain selected BC_5F_7 materials using CAPS molecular marker (**e**), PCR products of certain selected BC_5F_7 materials were digested using the endonuclease *Sac* II (**f**). **g** Morphology of ZM9023 and BBS plants at maturity stage, scale bar, 10 cm. **h-j** Aboveground dry weight (**h**), yield per plant (**i**), and grain N accumulation (**j**) of ZM9023 and BBS under NN or LN fields. *n* = 15 biological replicates for ZM9023 and BBS. In **a** and **h-j**, *P* values were generated from two-side Student's *t* tests. Source data are provided as a Source Data file.

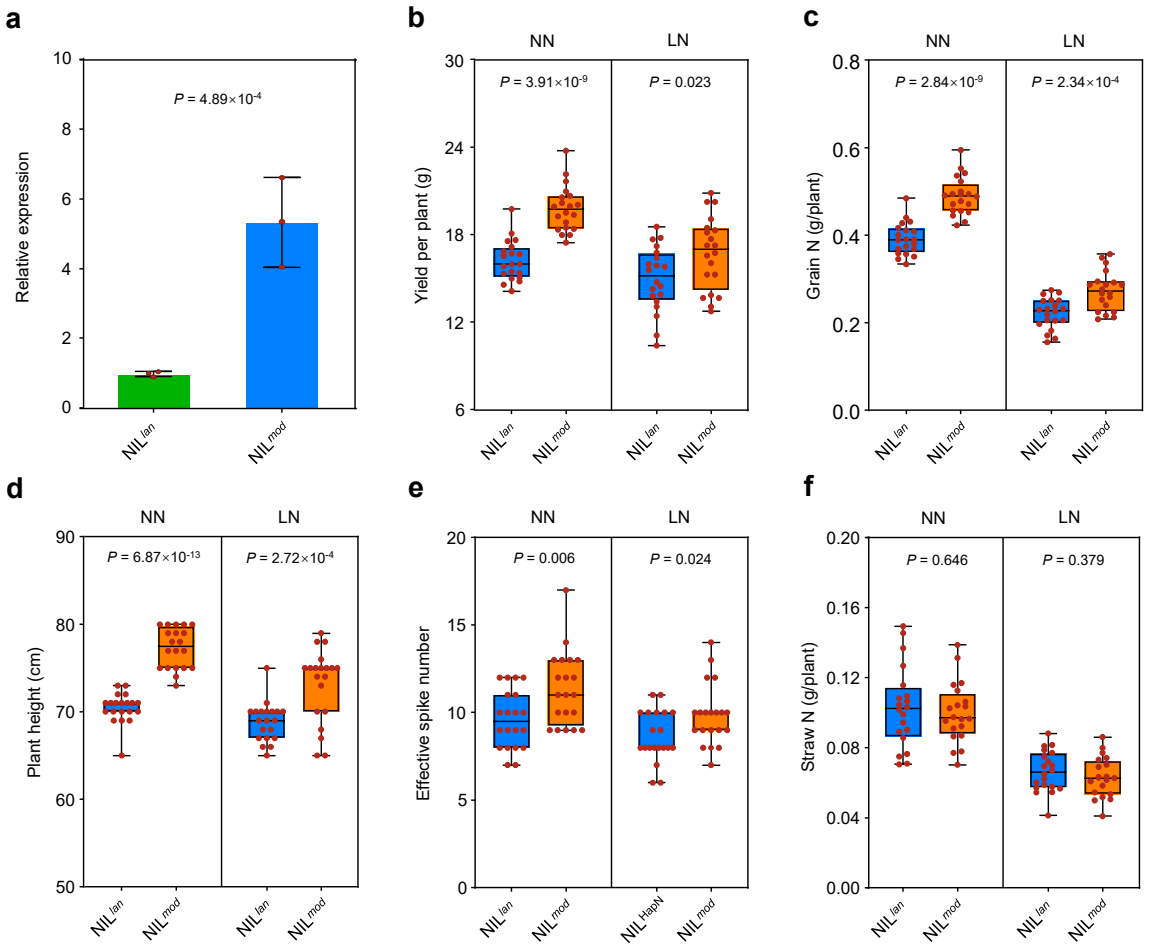

Supplementary Fig. 2 *TaNPF7.6-A1* expression levels and agronomic traits of the NILs under field conditions. a Relative expression of *TaNPF7.6-A1* in NIL^{lan} and NIL^{mod} lines. Three biological replicates for each experiment with *Taα-tubulin* as an internal control. **b-f** Yield per plant (**b**), grain N accumulation(**c**), plant height(**d**), effective spike number(**e**), straw N accumulation (**f**) in NIL lines. *n* = 20 plants. In **a-f**, *P* values were calculated with two-tailed Student's *t* test. Source data are provided as a Source Data file.

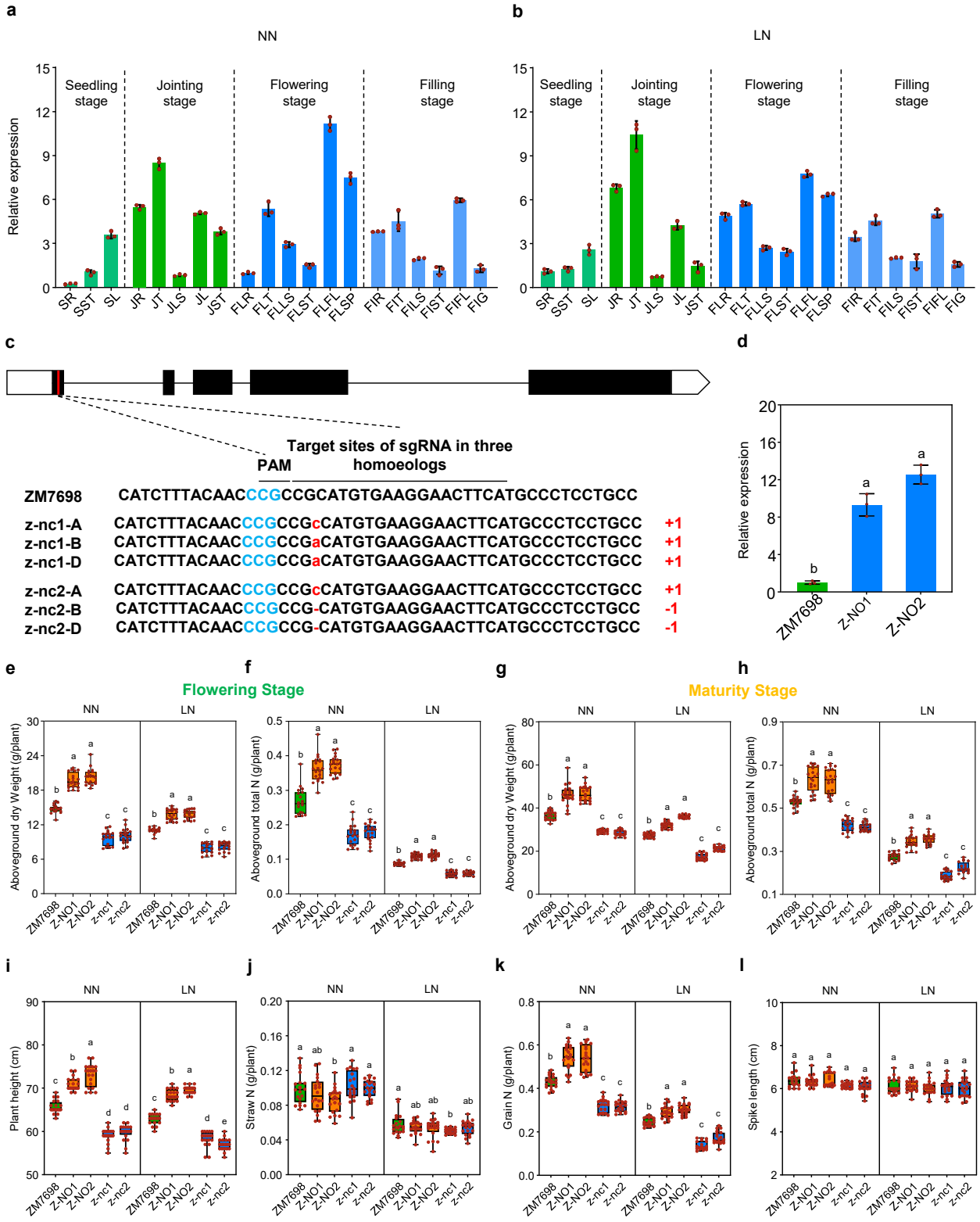

Supplementary Fig. 3 NUE-related traits of *TaNPF7.6-A1*^{mod} transgenic and CRISPR knockout lines under NN and LN fields. a-b Relative expression of *TaNPF7.6-A1*^{mod} in various wheat tissues at different stage under NN (**a**), and LN (**b**) fields. Tissues sampled include seedling root (SR), seedling stems (SST), seedling leaves (SL), roots, tiller basal part, leaf sheath, leaves and stems at jointing stage (JR, JT, JLS, JL, JST), roots, tiller basal part, leaf sheath, stems, flag leaves and spikes at flowering stage (FLR, FLT, FLLS, FLST, FLFL, FLSP), roots, tiller basal part, leaf sheath, stems, flag leaves at filling stage (FIR, FIT, FILS, FIST, FIFL) and developing grains at 20 DAP (FIG). Three biological replicates for each experiment with *Taα-tubulin* as an internal control. Data are presented as means ± S.D. **c** Mutations in the two *TaNPF7.6-A1* CRISPR knockout lines (z-nc1 and z-nc2 in the ZM7698 background). Black bars: the coding region; white bars: the UTRs; red lines: locations of the editing targets, and the locations of the mutants are described below.

d Relative expression of *TaNPF7.6-A1* in ZM7698 and overexpression lines in ZM7698 background. Values represent mean ± SD derived from shoot tissues from three individual wheat seedlings. **e-f** Aboveground dry weight (**e**), and aboveground total N (**f**), at the flowering stage in ZM7698, Z-NO and z-nc lines. n = 20 plants. **g-h** Aboveground dry weight (**g**), and aboveground total N (**h**) at the maturity stage in ZM7698, Z-NO and z-nc lines. n = 20 plants. **i-l** Plant height (**i**), straw N (**j**), Grain N (**k**) and spike length (**l**) at the maturity stage in ZM7698, Z-NO and z-nc lines. n = 20 plants. In **d-l**, different letters indicate significant differences ($P < 0.05$, one-way ANOVA, Duncan's new multiple range test). Source data are provided as a Source Data file.

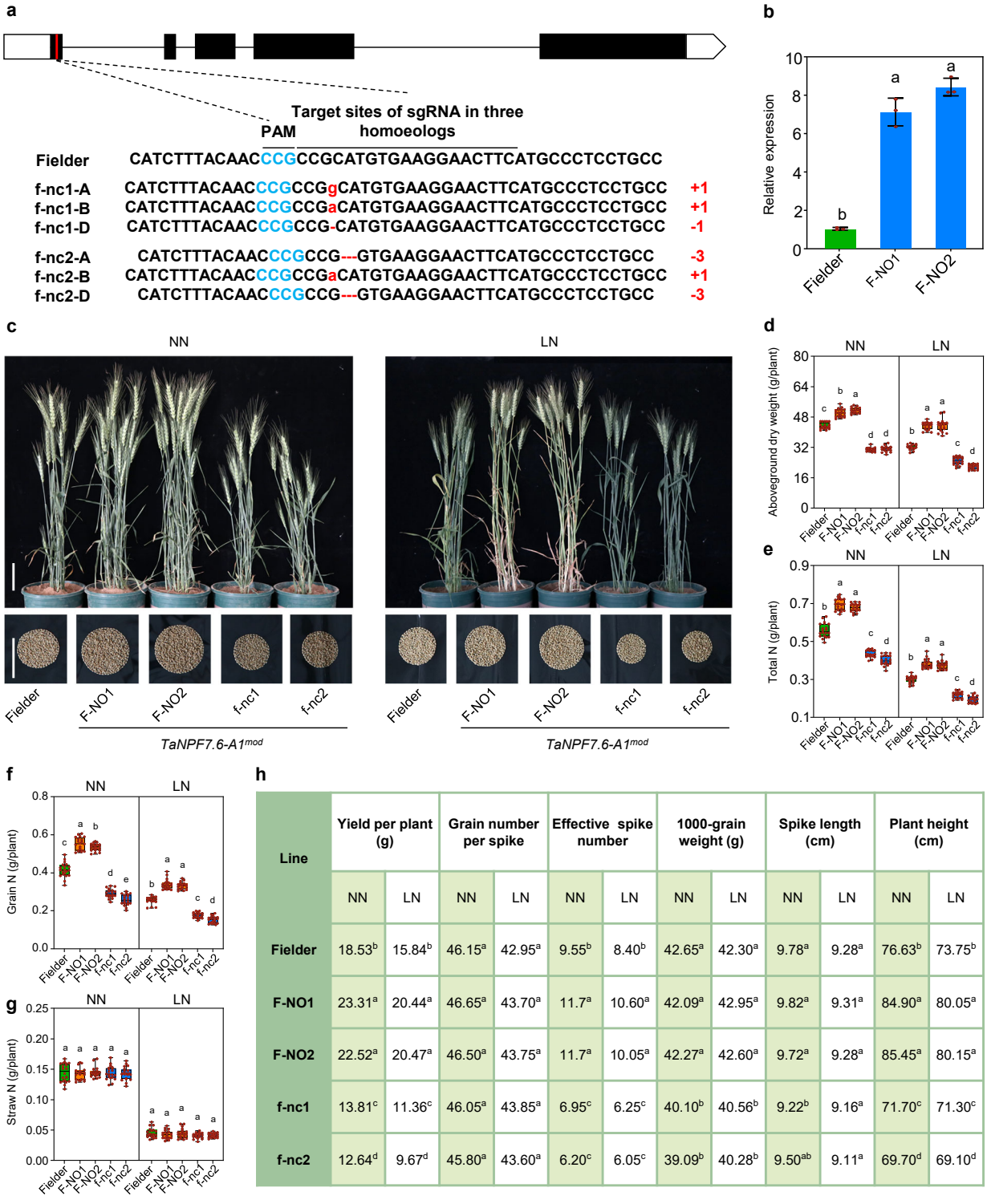

h

Line	Yield per plant (g)		Grain number per spike		Effective spike number		1000-grain weight (g)		Spike length (cm)		Plant height (cm)	
	NN	LN	NN	LN	NN	LN	NN	LN	NN	LN	NN	LN
Fielder	18.53^{b}	15.84^{b}	46.15^{a}	42.95^{a}	9.55^{b}	8.40^{b}	42.65^{a}	42.30^{a}	9.78^{a}	9.28^{a}	76.63^{b}	73.75^{b}
F-NO1	23.31^{a}	20.44^{a}	46.65^{a}	43.70^{a}	11.7^{a}	10.60^{a}	42.09^{a}	42.95^{a}	9.82^{a}	9.31^{a}	84.90^{a}	80.05^{a}
F-NO2	22.52^{a}	20.47^{a}	46.50^{a}	43.75^{a}	11.7^{a}	10.05^{a}	42.27^{a}	42.60^{a}	9.72^{a}	9.28^{a}	85.45^{a}	80.15^{a}
f-nc1	13.81^{c}	11.36^{c}	46.05^{a}	43.85^{a}	6.95^{c}	6.25^{c}	40.10^{b}	40.56^{b}	9.22^{b}	9.16^{a}	71.70^{c}	71.30^{c}
f-nc2	12.64^{d}	9.67^{d}	45.80^{a}	43.60^{a}	6.20^{c}	6.05^{c}	39.09^{b}	40.28^{b}	9.50^{ab}	9.11^{a}	69.70^{d}	69.10^{d}

Supplementary Fig. 4 *TaNPF7.6-A1*^{mod} positively regulates NUE and grain yield in wheat (Fielder background). a Mutations in the two *TaNPF7.6-A1* CRISPR knockout lines (f-nc1 and f-nc2 in the fielder background). Black bars: the coding region; white bars: the UTRs; red lines: locations of the editing targets, and the locations of the mutants are described below. **b** Relative expression of *TaNPF7.6-A1* in Fielder and overexpression lines in Fielder background. Values represent mean ± SD derived from shoot tissues from three individual wheat seedlings. **c** The phenotypes of Fielder, F-NO and f-nc lines at the maturity stage under LN and NN fields. Scale bars, 10 cm. **d-e** Aboveground dry weight (**d**) and aboveground total N (**e**) at the maturity stage in Fielder, F-NO and f-nc lines. n = 20 plants. **f-g** Grain N (**f**) and straw N (**g**) at the maturity stage in Fielder, F-NO and f-nc lines. n = 20 plants. **h** Agronomic traits of the wiid type (Fielder), F-NO lines and f-nc lines. In **b** and **d-h**, different letters indicate significant differences (P < 0.05, one-way ANOVA, Duncan's new multiple range test). Source data are provided as a Source Data file.

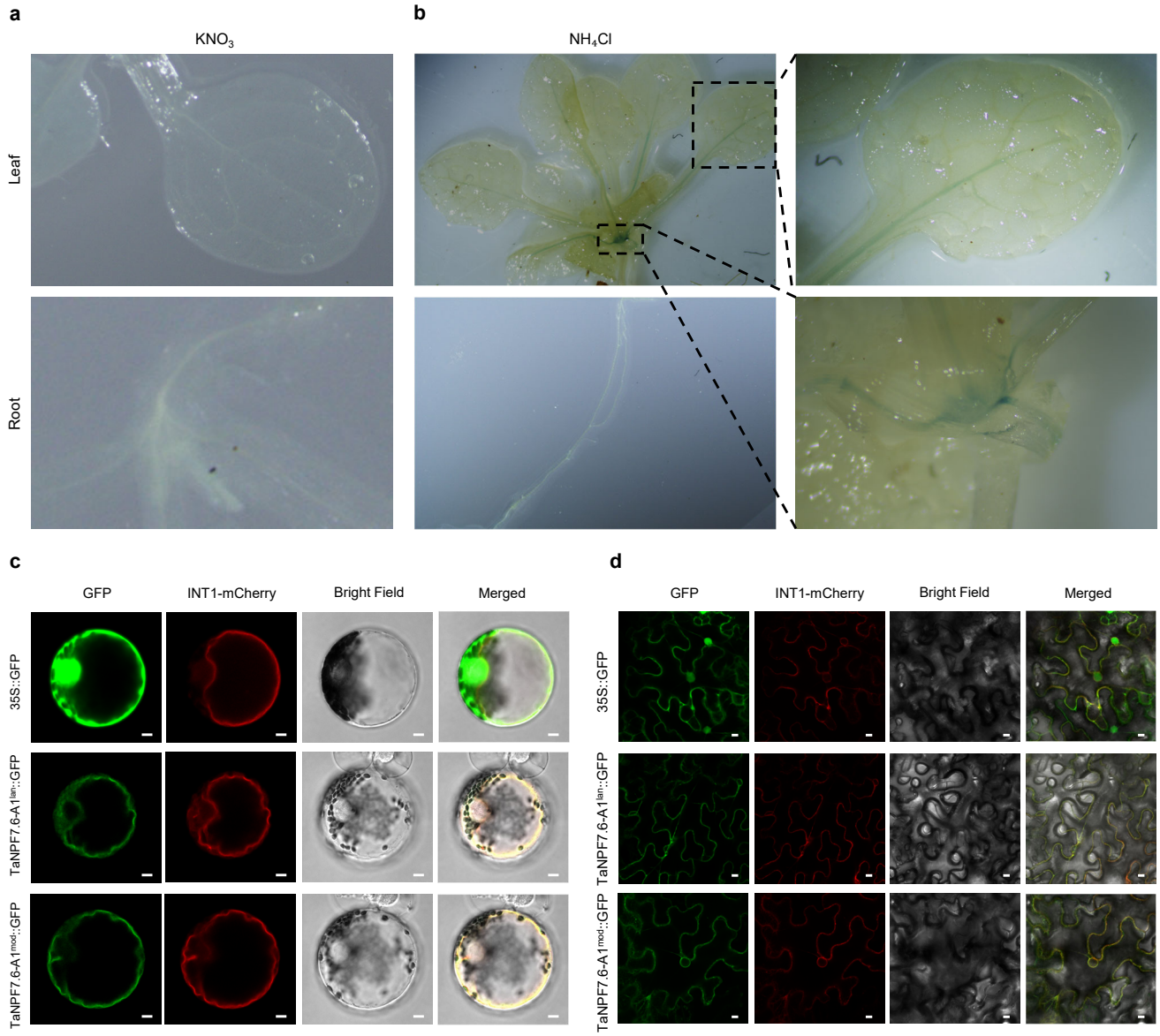

Supplementary Fig. 5 GUS analysis and subcellular localization of *TaNPF7.6-A1*. a-b GUS analysis of *TaNPF7.6-A1*^{mod} promoter in 1-week-old transgenic *Arabidopsis thaliana* seedlings grown on 1/2MS medium supplemented with 2 mM NH_4Cl (**a**), or 2 mM KNO_3 (**b**) as the sole nitrogen source. **c-d** Subcellular localization indicated that TaNPF7.6-A1^{lan} and TaNPF7.6-A1^{mod} (fused with GFP) was localized to the vacuole membrane (co-localized with AtINT1 fused with mCherry) in wheat protoplasts (**c**), and *N. benthamiana* leaves (**d**), free GFP was used as a control, scale bars = 10 μm.

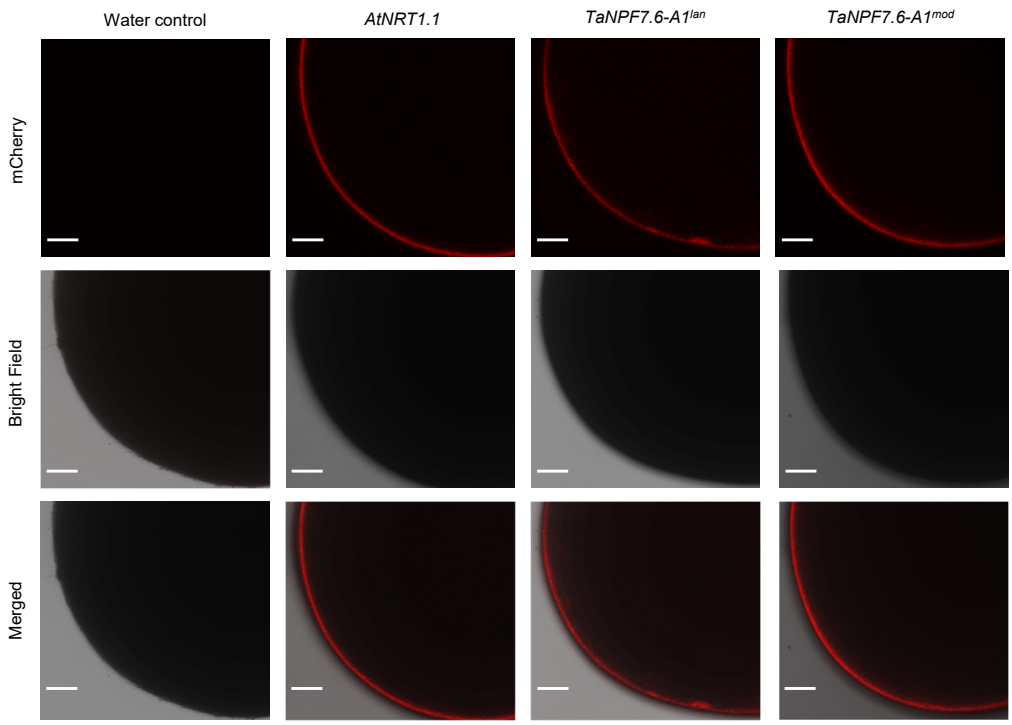

Supplementary Fig. 6 The expression of two *TaNPF7.6-A1* alleles and *AtNRT1.1* fused with mCherry or a water control, was examined in *Xenopus laevis* oocytes. *TaNPF7.6-A1*^{lan} and *TaNPF7.6-A1*^{mod} (fused with mCherry) were correctly expressed in *Xenopus laevis* oocytes, *AtNRT1.1* was used as the positive control, water was used as the negative control, scale bars = 100 μm.

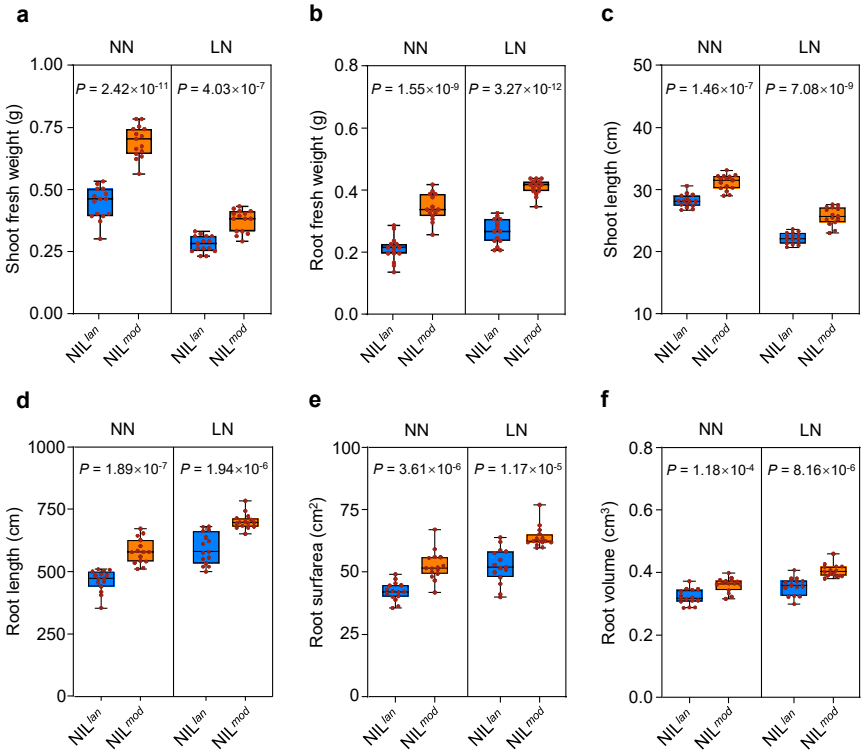

Supplementary Fig. 7 Growth parameters of the NIL^{lan} and NIL^{mod} lines hydroponically grown under NN (2 mM nitrate) and LN (0.2 mM nitrate) conditions. a-f Shoot fresh weight (**a**), root fresh weight (**b**), shoot length (**c**), total root length (**d**), root surface area (**e**), root volume (**f**) of the NIL^{lan} and NIL^{mod} lines. Wheat seedlings were grown for 14 d in a different nutrient solution (NN and LN); the roots were then scanned with an STD1600 scanner and analyzed for root morphological parameters with WinRHIZO software (Regent Instrument Inc.). In **a-f** n = 15 biological replicates for NIL^{lan} and NIL^{mod}. P values were calculated with two-tailed Student's t test. Source data are provided as a Source Data file.

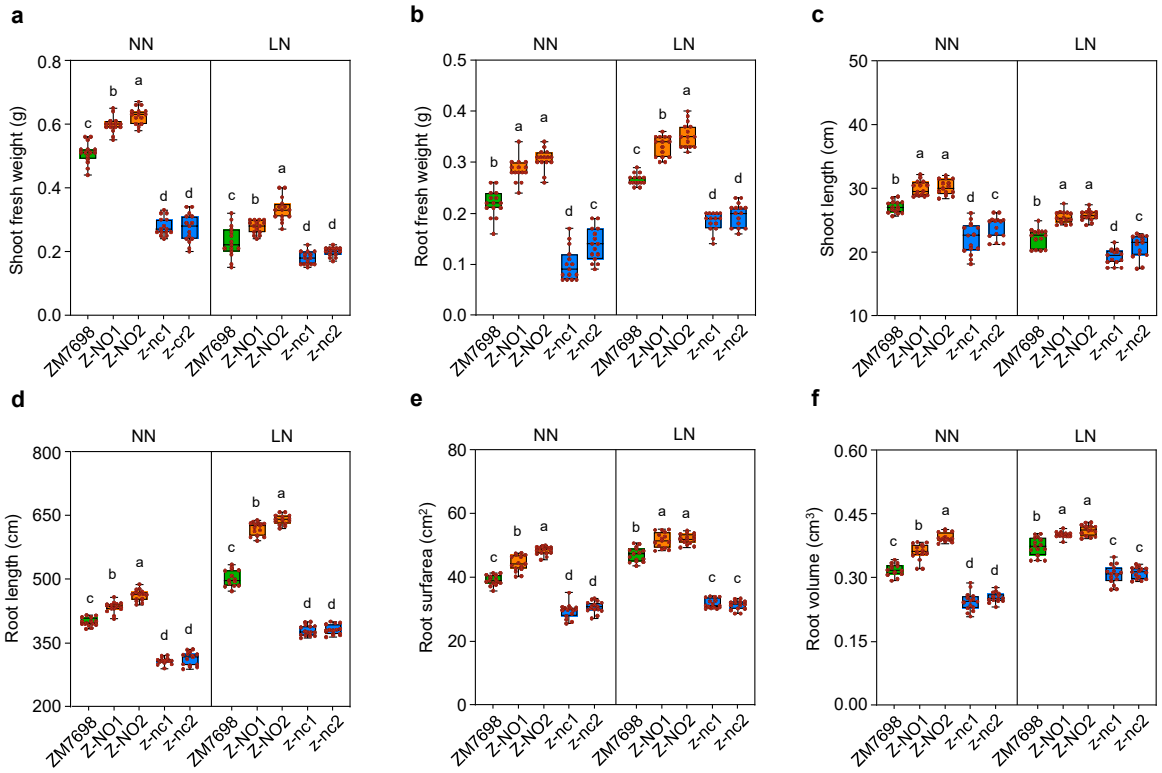

Supplementary Fig. 8 Growth parameters of the ZM7698, Z-NO and z-nc lines hydroponically grown under NN (2 mM nitrate) and LN (0.2 mM nitrate) conditions. a-f Shoot fresh weight (**a**), root fresh weight (**b**), shoot length (**c**), total root length (**d**), root surface area (**e**), root volume (**f**) of ZM7698, Z-NO1, Z-NO2, z-nc1 and z-nc2. Wheat seedlings were grown for 14 d in a different nutrient solution; the roots were then scanned with an STD1600 scanner and analyzed for root morphological parameters with WinRHIZO software (Regent Instrument Inc.). n = 15 biological replicates. In **a-f**, different letters indicate significant differences (P < 0.05, one-way ANOVA, Duncan's new multiple range test). Source data are provided as a Source Data file.

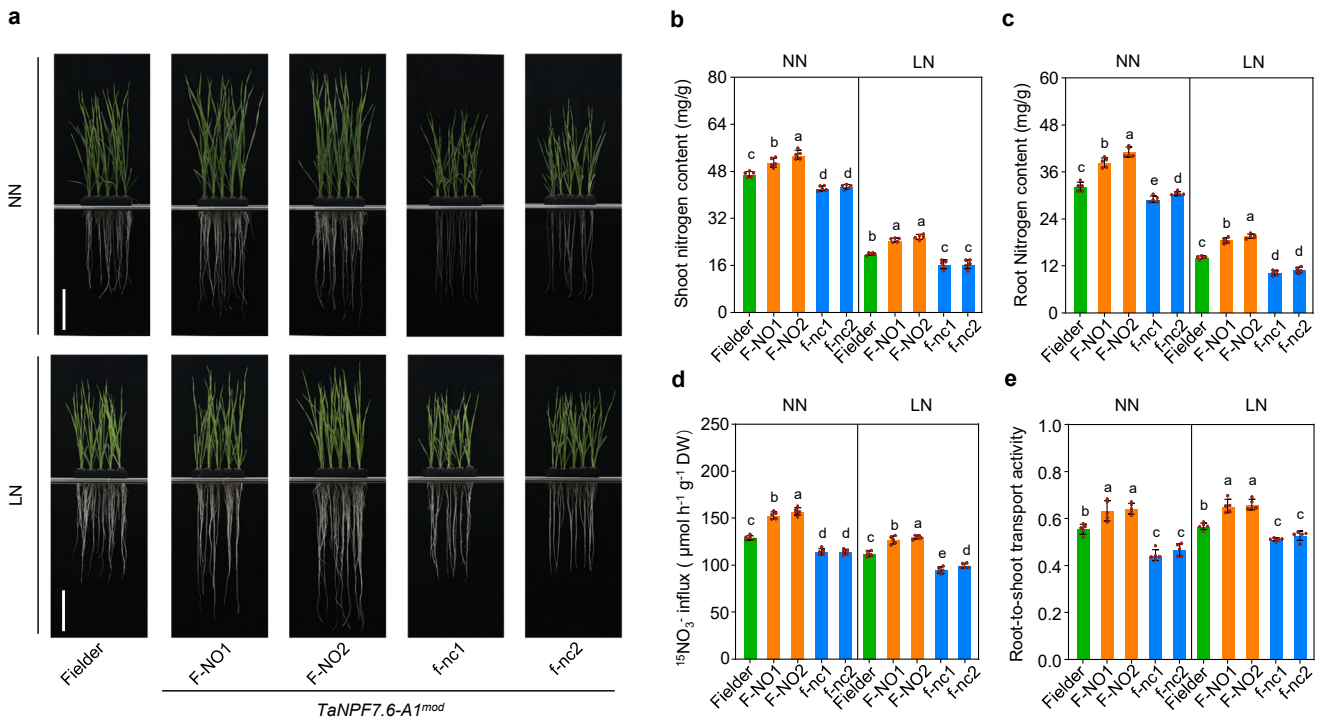

Supplementary Fig. 9 ***TaNPF7.6-A1*** ^{mod} **positively regulates wheat nitrate uptake and translocation capacity (Fielder background). a** Growth of Fielder, F-NO and f-nc lines in 2-week hydroponic culture under NN (2 Mm nitrate) or LN (0.2 Mm nitrate) conditions, scale bar = 10 cm. **b-c** Total nitrogen content of shoots (**b**) and roots (**c**) of Fielder, F-NO and f-nc lines in 2-week hydroponic culture under NN (2 Mm nitrate) or LN (0.2 Mm nitrate) conditions. **d-e** $^{15}N–NO_3^-$ uptake (**d**) and root-to-shoot transport activities (**e**) of Fielder, F-NO and f-nc lines when exposed to either NN (2 Mm nitrate) or LN (0.2 Mm nitrate) ^{15}N-labeled KNO_3 for 3 h. In **b-e,** data are mean ± SD (n=5 biological replicates for Fielder, F-NO1, F-NO2, f-nc1 and f-nc2. Different letters indicate significant differences ($P < 0.05$, one-way ANOVA, Duncan's new multiple range test). Source data are provided as a Source Data file.

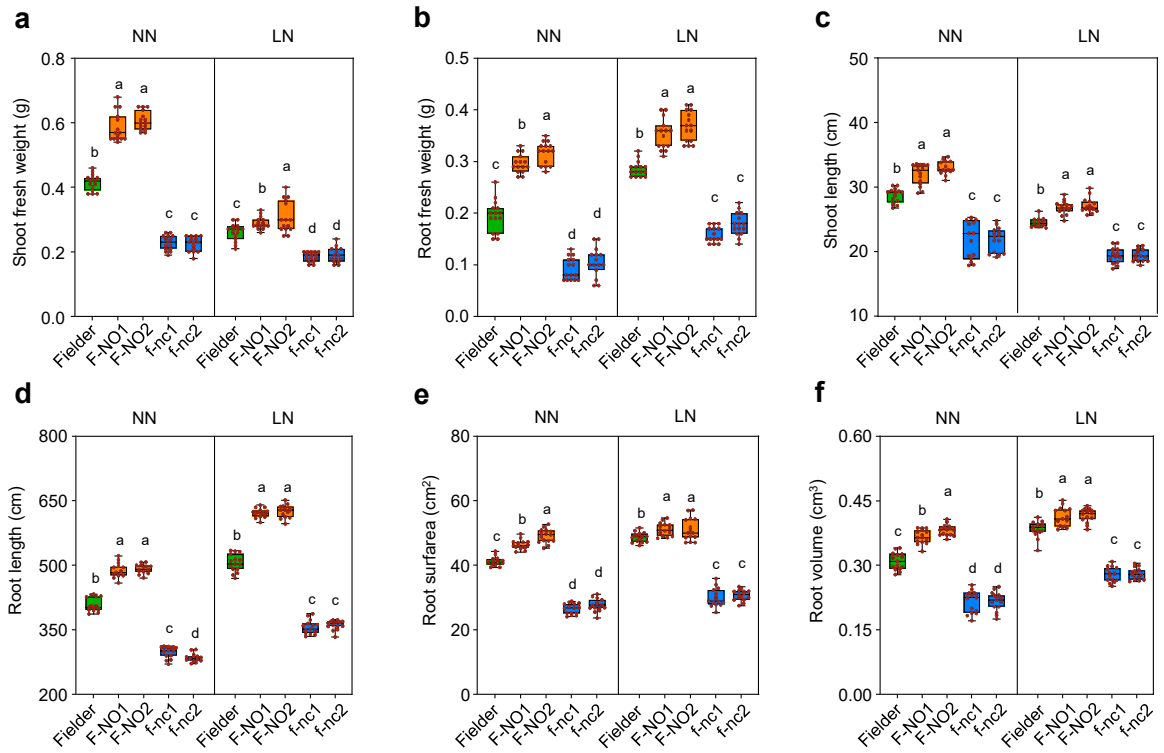

Supplementary Fig. 10 Growth parameters of the Fielder, F-NO and f-nc lines hydroponically grown under NN (2 mM nitrate) and LN (0.2 mM nitrate) conditions. a-f Shoot fresh weight (**a**), root fresh weight (**b**), shoot length (**c**), total root length (**d**), root surface area (**e**), root volume (**f**) of Fielder, F-NO1, F-NO2, f-nc1 and f-nc2. Wheat seedlings were grown for 14 d in a different nutrient solution; the roots were then scanned with an STD1600 scanner and analyzed for root morphological parameters with WinRHIZO software (Regent Instrument Inc.). n = 15 biological replicates. Different letters indicate significant differences ($P < 0.05$, one-way ANOVA, Duncan's new multiple range test). Source data are provided as a Source Data file.

a

Haplotype	Promoter								
	V1	V2	V3	V4	V5	V6	V7	V9	V10
	-1640	-1603	-1216	-777	-761	-749	-719	-542	-522
TaNPF7.6-A1^{lan}	C	G	C	C	C	G	A	A	C
TaNPF7.6-A1^{mod}	T	A	A	T	T	T	G	G	T

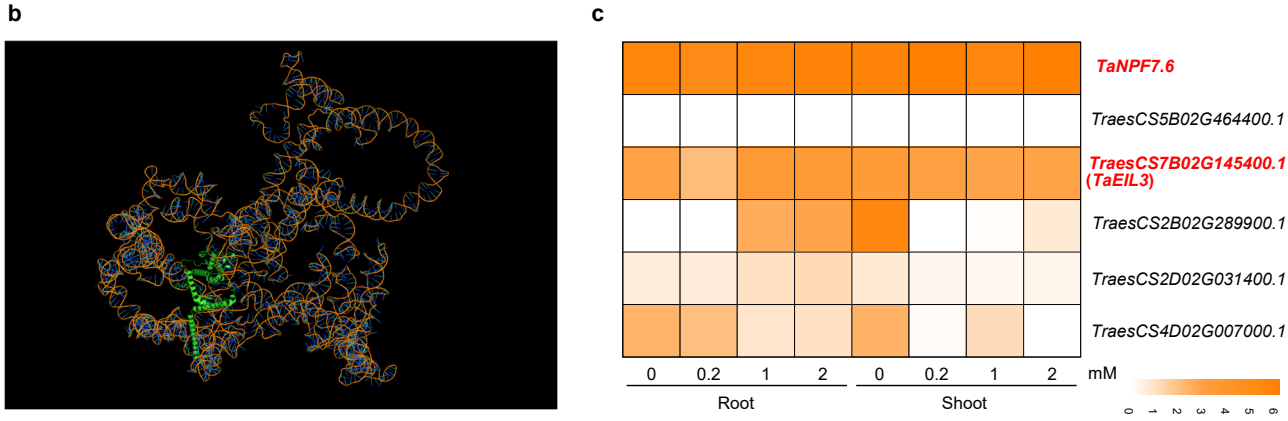

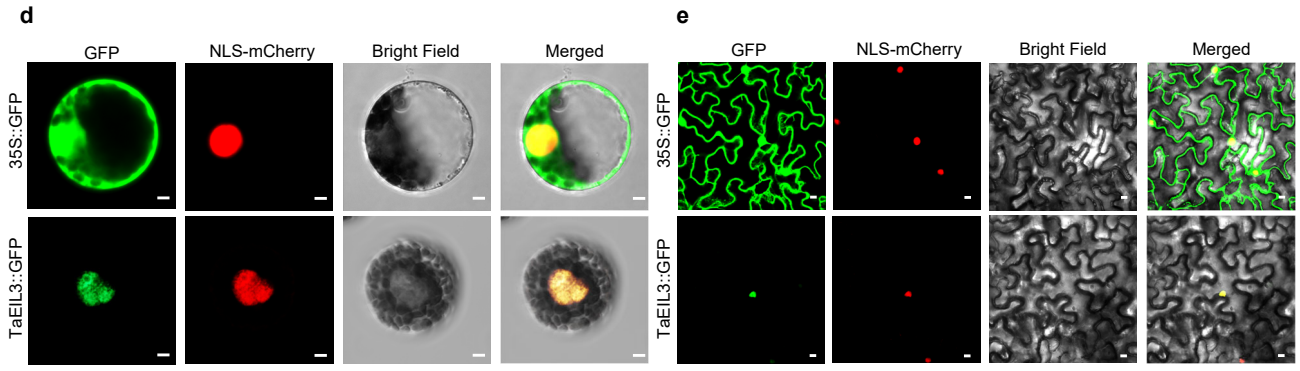

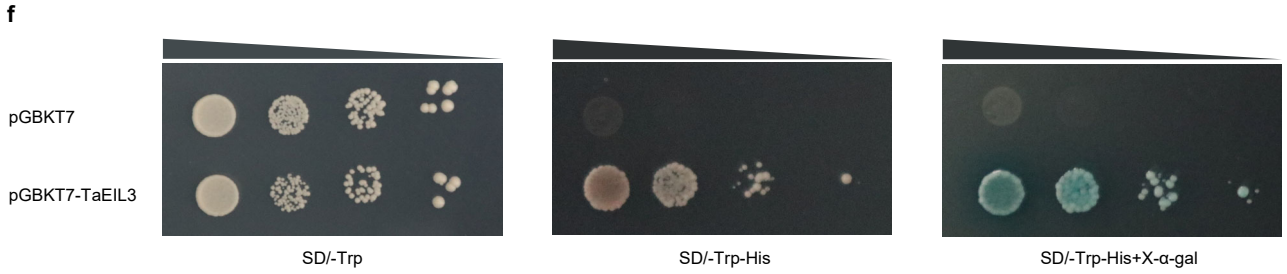

Supplementary Fig. 11 Analysis of expression patterns of TaEIL3. a Schematic diagram showing the polymorphism on *TaNPF7.6-A1* promoter that dividing *lan* and *mod* in twenty wheat varieties. **b** 3D model of the TaEIL3-*TaNPF7.6-A1^{mod} pro* module predicted via AlphaFold. **c** Heatmap representation of expression levels for five candidate genes under four nitrogen supply conditions (0, 0.2, 1, and 2 mM NO_3^-) based on RNA sequencing of roots and shoots of wheat seedlings. **d-e** Subcellular localization of TaEIL3 in wheat protoplasts (**d**), and *N. benthamiana* leaves (**e**), a nuclear localization signal (NLS, MDPKKKRKV) protein fused with red fluorescent protein mCherry was used as a nuclear marker, scale bars = 10 μm. **f** The TaEIL3-BD vector was transformed into yeast strains alone, which showed that it could grow on SD medium lacking Trp and His.

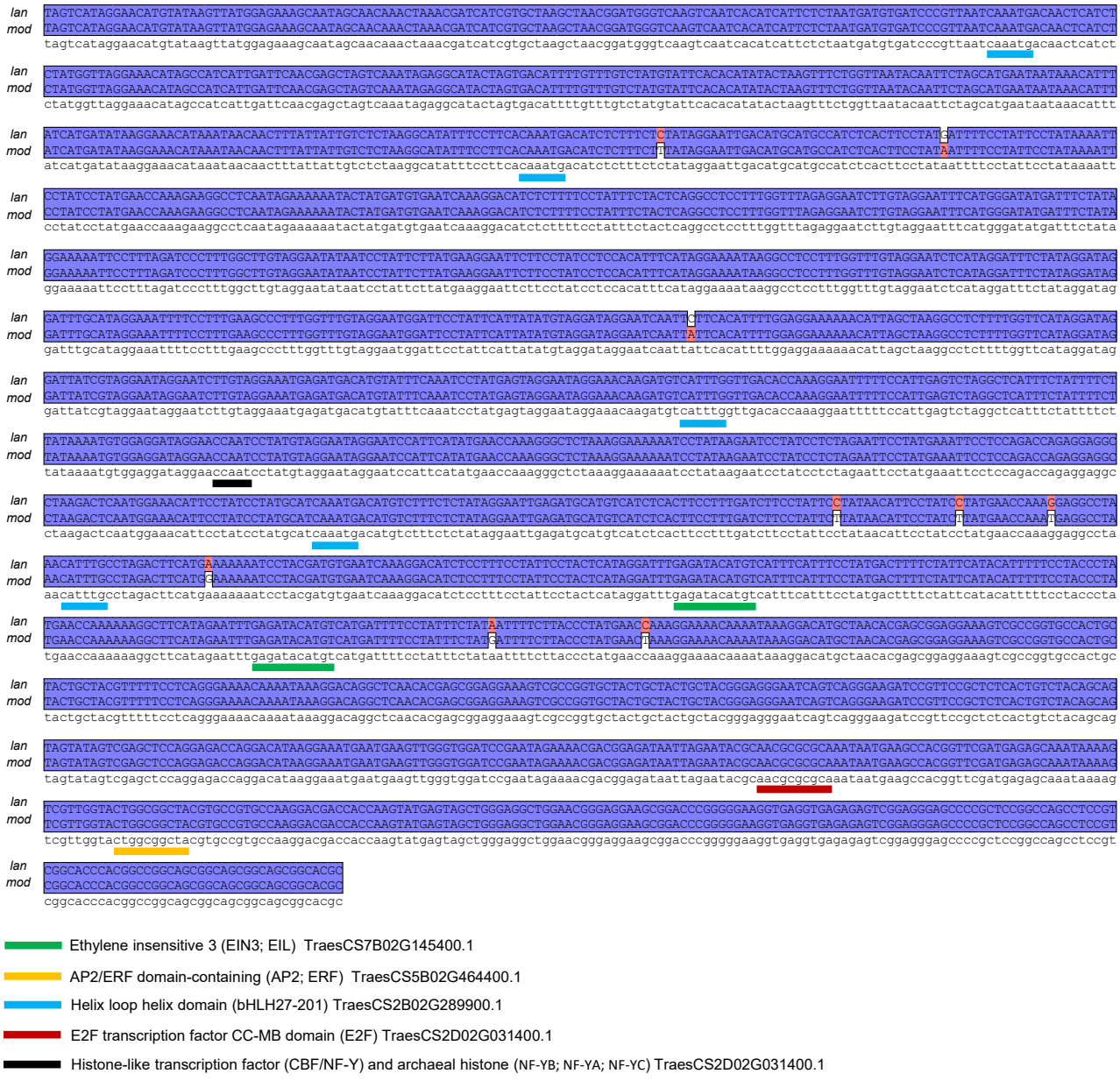

Supplementary Fig. 12 Nucleotide sequence comparison of the *TaNPF7.6-A1*^{mod} and *TaNPF7.6-A1*^{lan} promoters. The nucleotide sequences of the *TaNPF7.6-A1*^{mod} and *TaNPF7.6-A1*^{lan} promoters and the potential consensus sequences for the regulatory elements.

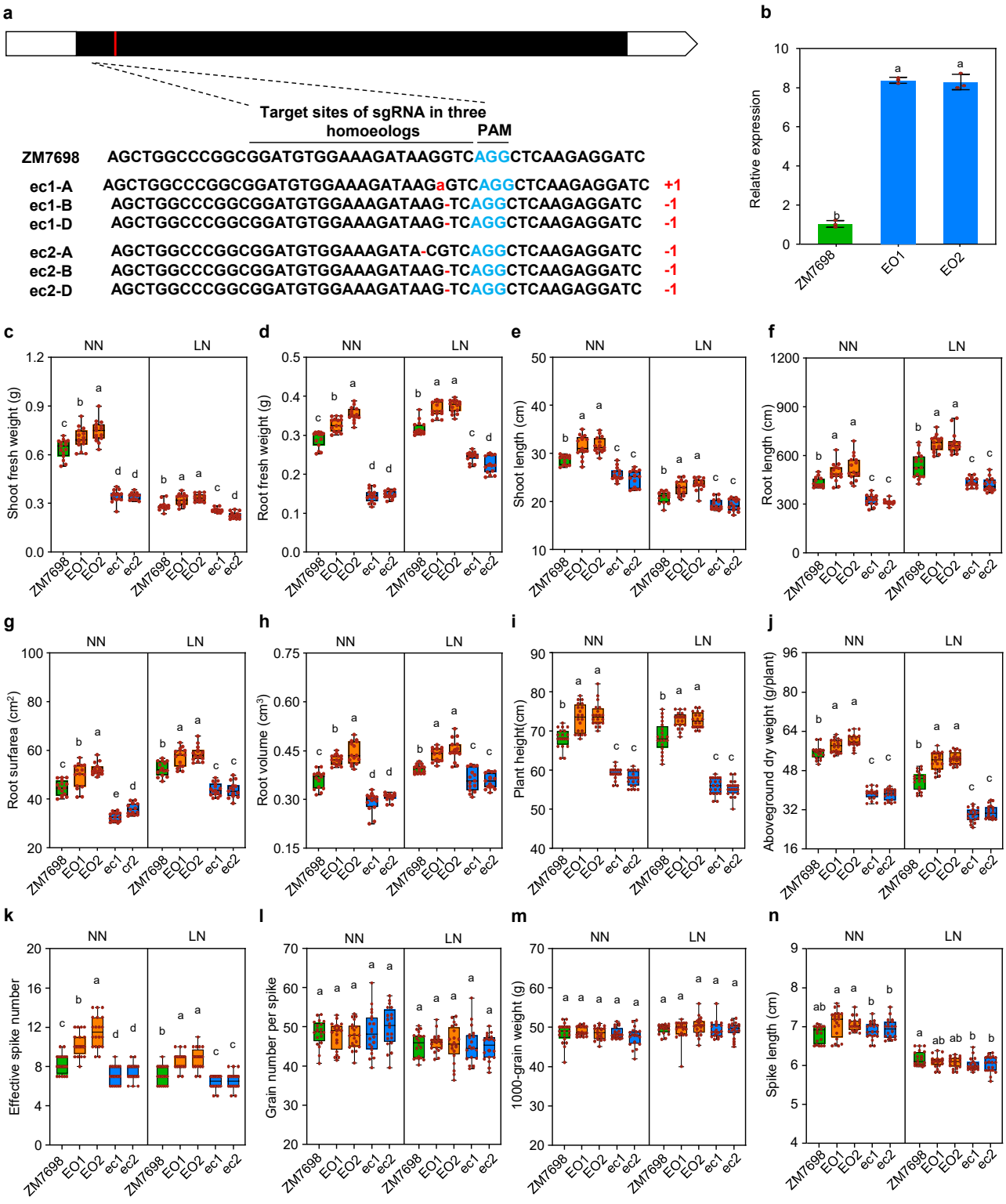

Supplementary Fig. 13 Identification of *TaEIL3* overexpression (EO) and *TaEIL3* knockout (ec) lines. a The mutation in the *TaEIL3* CRISPR/Cas9 knockout lines in the ZM7698 background. Black bars: the coding region; white bars: the UTRs; red lines: locations of the editing targets, and the locations of the mutants are described below. **b** Relative expression of *TaEIL3* in ZM7698 and EO lines. *Taα-tubulin* was used as an internal control. **c-h** Shoot fresh weight (**c**), root fresh weight (**d**), shoot length (**e**), total root length (**f**), root surface area (**g**), root volume (**h**) of ZM7698, EO lines and ec lines hydroponically grown under NN (2 mM nitrate) and LN (0.2 mM nitrate) conditions, n = 15 biological replicates. **i-n** Plant height (**i**), aboveground dry weight (**j**), effective spike number(**k**), grain number per spike (**l**), 1000-grain weight (**m**) and spike length (**n**) at the maturity stage in ZM7698, EO and ec lines. n = 20 plants. In **b**-**n**, different letters indicate significant differences (P < 0.05, one-way ANOVA, Duncan's new multiple range test). Source data are provided as a Source Data file.

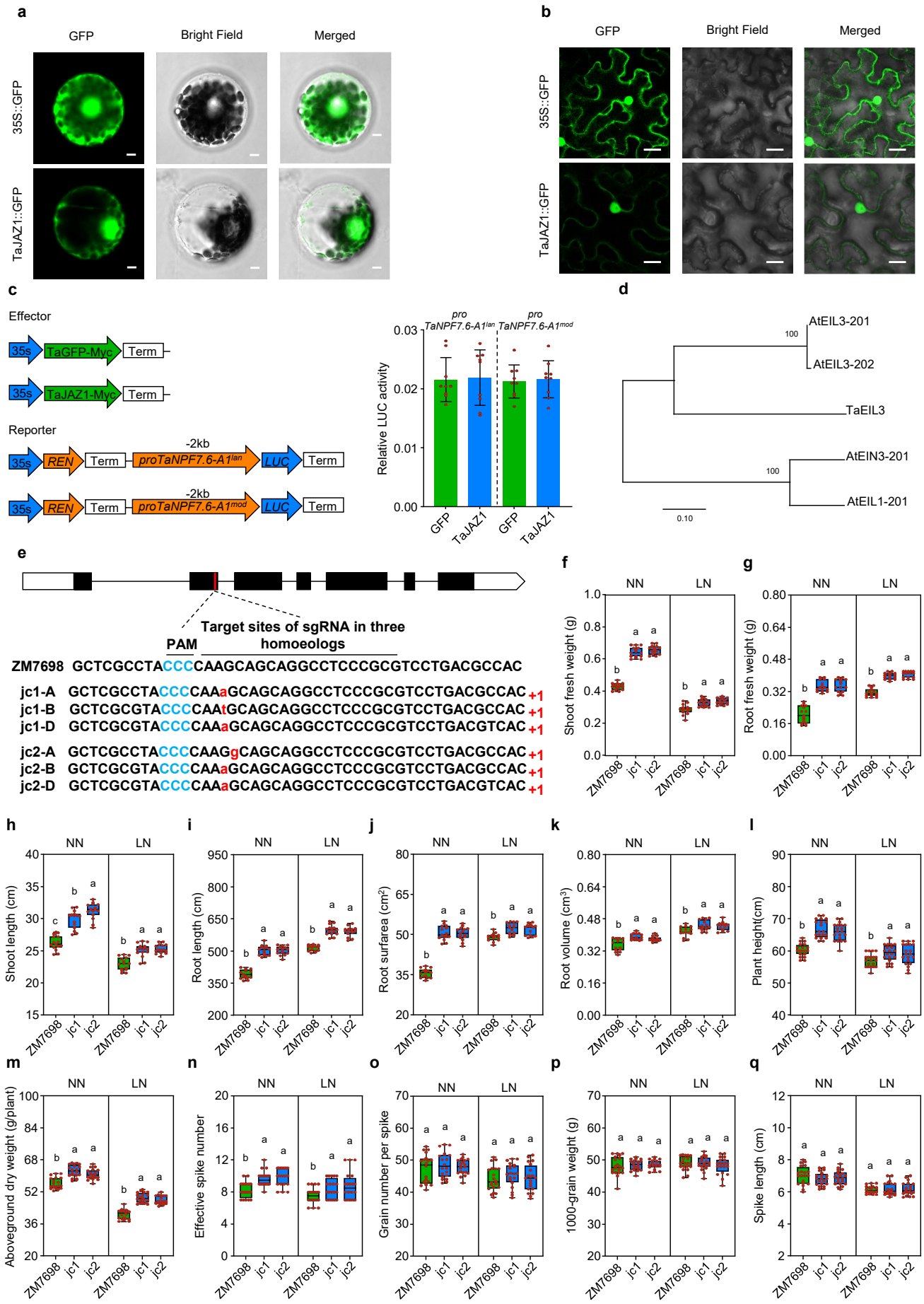

Supplementary Fig. 14 Subcellular localization of TaJAZ1 and identification of *TaJAZ1* knockout materials. a-b Subcellular localization of TaJAZ1 in wheat protoplasts (**a**), and *N. benthamiana* leaves (**b**). **c** Transient activation assay of the *proTaNPF7.6-A1^{lan}-LUC* and *proTaNPF7.6-A1^{mod}-LUC* reporters in the leaves of *N. benthamiana* co-transformed with the indicated TaJAZ1 or GFP effector

constructs. **d** Phylogenetic tree analysis of TaEIL3, the scale represents the branch length. **e** The mutation in the *TaJAZ1* CRISPR/Cas9 knockout (jc) lines in the ZM7698 background. Black bars: the coding region; white bars: the UTRs; red lines: locations of the editing targets, and the locations of the mutants are described below. **f-k** Shoot fresh weight (**f**), root fresh weight (**g**), shoot length (**h**), total root length (**i**), root surface area (**j**), root volume (**k**) of ZM7698 and jc lines hydroponically grown under NN (2 mM nitrate) and LN (0.2 mM nitrate) conditions, n = 15 biological replicates. Different letters indicate significant differences ($P < 0.05$, one-way ANOVA, Duncan's new multiple range test). **l-q** Plant height (**l**), aboveground dry weight (**m**), effective spike number(**n**), grain number per spike (**o**), 1000-grain weight (**p**) and spike length (**q**) at the maturity stage in ZM7698, EO and ec lines. In **f-q,** n = 20 plants. Different letters indicate significant differences ($P < 0.05$, one-way ANOVA, Duncan's new multiple range test). Source data are provided as a Source Data file.

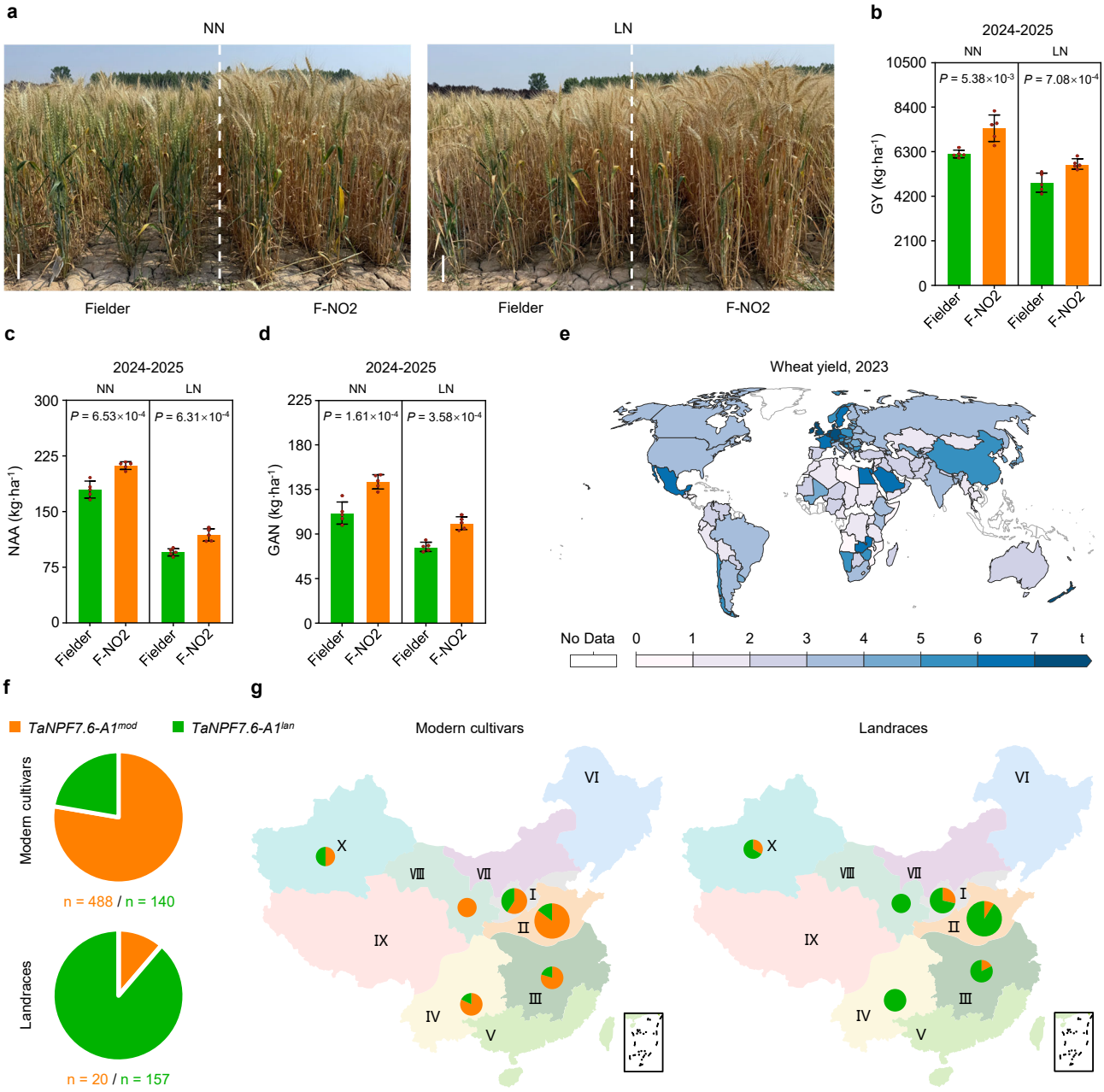

Supplementary Fig. 15 Breeding potential and allele distribution of *TaNPF7.6-A1* in China's wheat regions. a The phenotypes of Fielder and F-NO-2 line under LN and NN field at high planting densities. **b-d** Comparison of the GY(**b**), NAA(**c**) and GAN(**d**) between Fielder and F-NO-2 line at high planting densities under NN and LN field in 2024-2025. In **b-d**, *P* values were calculated with two-tailed Student's *t* test. Source data are provided as a Source Data file. **e** Global wheat yield in 2023, yields are the amount of crop harvested per unit area of land, they are measured in tonnes per hectare. (Data source: Food and Agriculture Organization of the United Nations, https://ourworldindata.org/). **f** Frequency distribution of *TaNPF7.6-A1*^{mod} and *TaNPF7.6-A1*^{lan} in 805 Chinese wheat. accessions (177 landraces and 628 modern cultivars). **g** Distribution analysis of *TaNPF7.6-A1*^{mod} and *TaNPF7.6-A1*^{lan} in China's wheat regions. $n = 805$ (177 landraces and 628 modern cultivars). I to X represent China's wheat 10 agroecological zones. I, northern winter wheat region; II, Yellow and Huai River valley winter wheat region; III, low and middle Yangtze River valley winter wheat region; IV, southwestern winter wheat region; V, southern winter wheat region; VI, northeastern spring wheat region; VII, northern spring wheat region; VIII, northwestern spring wheat region; IX, Qinghai-Tibet spring–winter wheat region; and X, Xinjiang winter–spring wheat region.